New Journal of Physics
The open–access journal for physics

Slow waves caused by cuts perpendicular to a single subwavelength slit in metal

J R Suckling and J R Sambles
Thin Film Photonics Group, School of Physics, Exeter University, Devon, EX4 4QL, UK
E-mail: j.r.sambles@exeter.ac.uk

New Journal of Physics **9** (2007) 1
Received 14 August 2006
Published 16 January 2007
Online at http://www.njp.org/
doi:10.1088/1367-2630/9/1/001

Abstract. Resonant transmission of microwaves through a subwavelength slit in a thick metal plate, into which subwavelength cuts have been made, is explored. Two orientations of the cuts, parallel and perpendicular to the long axis of the slit, are examined. The results show that the slits act as though filled with a medium with anisotropic effective relative permeability which at low mode numbers has the two values $\sim(1,\ 9.1)$, increasing to $\sim(1, 14.4)$ for higher mode numbers.

The study of transmission of photons through subwavelength apertures is an area of much current interest. Part of this study has focused on arrays of subwavelength slits [1]–[3], where it has been shown that there are two primary mechanisms for resonant transmission: either by coupling of resonant surface plasmon states from one surface through to the other or by the formation of Fabry–Perot-like resonances within the individual slits (equivalently the modes of a finite length waveguide) [1]. Fabry–Perot-like resonant transmission through periodic slit arrays has also been demonstrated in the microwave regime [4, 5]. Furthermore, it has been shown, both theoretically and experimentally, that a single, very subwavelength single slit in metal, illuminated with perpendicularly polarized photons, supports such Fabry–Perot-like resonances [6, 7]. The frequencies of the resonant modes are dependent on the separation of the metal plates [6, 8, 9] and the electromagnetic properties of the bounding metal [8, 10].

Here we explore the effect of making cuts into the metal, both parallel and perpendicular to the long axis of the slit, arranged in a subwavelength pitch array. It is shown that the presence of the cuts modifies the electromagnetic properties of the slit, making it appear as though filled with a material with an enhanced refractive index for waves propagating in a direction perpendicular to that of the cuts and with magnetic fields in the slit plane. This effect is due to the formation of current loops in the plane lying perpendicular to the cuts resulting in an enhanced effective relative

PII: S1367-2630(07)30663-0

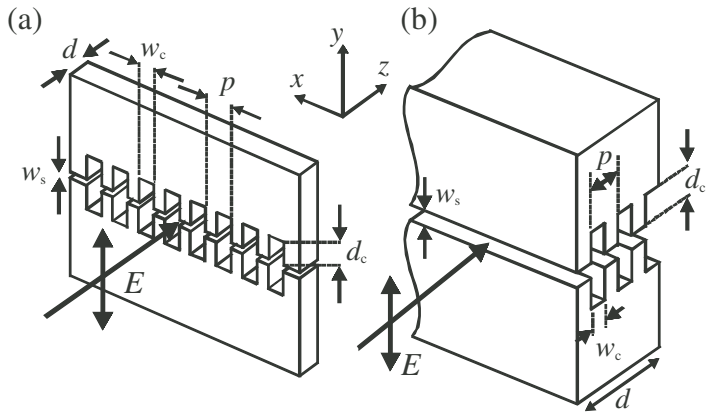

Figure 1. (a) Sample with cuts made perpendicular to the long axis of the slit. (b) Sample with cuts made parallel to the long axis of the slit; dimensions and incident beam marked. Axes correspond to computer model.

permeability of the space inside the slit. This enhancement is shown to be highly dependent on the separation of the plates. Numerical values are presented for the relative permeability at various plate separations, and a maximum experimental value of $\mu = 14.4$ ($n = 3.8$) is found for a plate separation of $50\,\mu$m for high order resonant modes.

Simple Fabry–Perot theory for the resonant frequencies f_{FP} of a cavity formed by a slit in a metal plate of thickness, d, filled with a dielectric of refractive index n, gives

$$f_{FP} = \frac{cN}{2nd} \tag{1}$$

where N is the resonant order number and c the speed of light in vacuum. The lowest resonant frequency supported within a vacuum-filled slit has a wavelength corresponding to twice the thickness of the plate. In reality, the resonant frequency of any mode within the open ended slit is lower than this simple prediction, either due to the expansion of the fields out of the slit [6] or the penetration of the fields into the metal [8]. However, these shifts are small relative to the resonant frequencies, of the order of a few per cent; larger changes in resonant frequency require modification of the slit cavity, for example a change of dielectric in the cavity [10, 11] or, as in this study, the introduction of cuts into the slit walls.

Two slit structures were studied, as shown in figure 1(a) and (b). Both slit structures are formed from a gap between two large plates of aluminum, such that the whole face area ($\sim$400 $\times$ 200 mm) is much larger than the incident microwave beam area. The two plates are separated by dielectric spacers (which are placed outside the incident microwave beam), thereby defining the slit width, w_s, which is varied over the range $30 < w_s < 1000\,\mu$m. In sample (a), figure 1(a), cuts are made perpendicular to the long axis of the slit. These cuts have a depth $d_c = 1.48$ mm, width $w_c = 0.84$ mm and pitch $p = 1.2$ mm. The overall depth of the slit is 19.63 mm. In sample (b), figure 1(b), cuts are made into the metal parallel to the long axis of the slit. These cuts have a depth, $d_c = 0.5$ mm, width, $w_c = 0.91$ mm and pitch, $p = 2$ mm. The overall depth of this resonant slit structure is 20.01 mm. These slit structures are then placed individually between two microwave horns, one acting as a source and the other as a detector, with the detector horn placed $\sim$10 cm distance from the plate, far enough away not to be considered

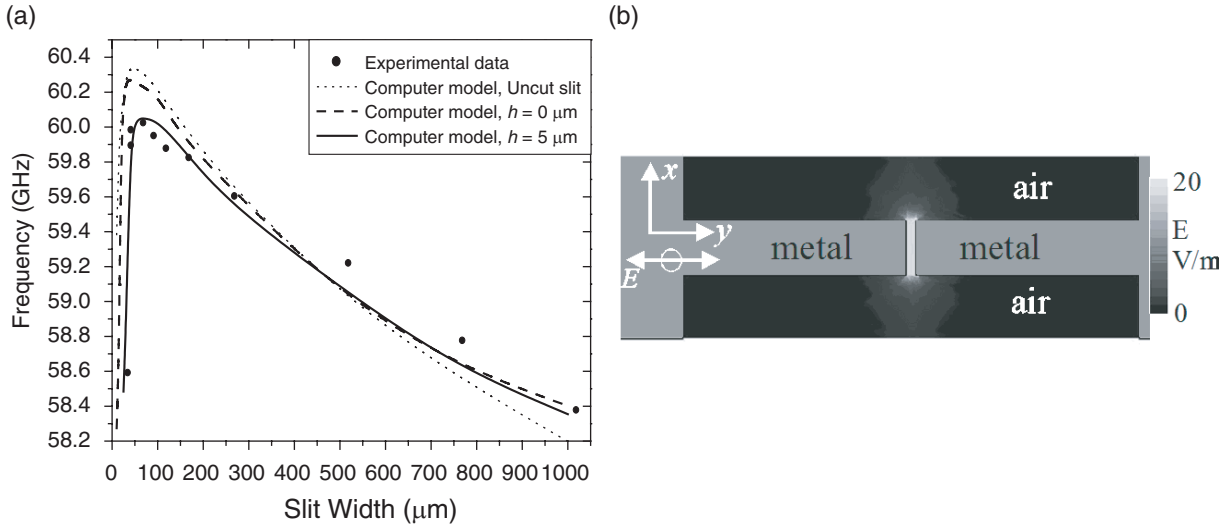

Figure 2. (a) Resonant frequency of the $N = 8$ mode for sample (a) as a function of slit width over the range $16 < w_s < 1000\,\mu$m. Data from perpendicular cut sample (dots), computer model with smooth metal (dashed line), rough surface with mean roughness $h = 5\,\mu$m (solid line) and slit in uncut metal (dotted line) are shown. (b) The electric field amplitude for the $N = 8$ resonance within a rough sample (a) with a slit width of 73 μm. Fields are shown in the x–y plane 10 mm inside the slit. The electric field is enhanced by a factor of ~20 inside slit.

near-field, yet as close as possible to give acceptable signals from the very narrow slits. The horns are also aligned such that the incident microwaves are polarized perpendicular to the slit. Transmission through the slit is observed over the frequency range $4.6 < f < 75$ GHz (λ ranging from 65 to 4 mm), the structures within the slits being subwavelength at all experimental frequencies.

Figure 2(a) shows the resonant response of the $N = 8$ mode within sample (a) as a function of slit width over the range $36 < w_s < 1000\,\mu$m. The experimental data are shown as dots. The form of the data is very similar to that of figure 2, [8], with the resonant frequency being a maximum at a slit width of ~50 μm, decreasing in frequency as the slit width both increases and decreases away from 50 μm. Three outputs of a finite element modelling (FEM) program, Ansoft's High Frequency Structure Simulator [12], are shown as the solid, dashed and dotted lines. The dashed line is the predicted response of a model whose dimensions are the same as the experimental sample, with metal that has a perfectly smooth surface. It is clear that the resonant frequency of the model with the perfectly smooth metal is very similar to that of a slit in an otherwise uncut metal plate, whose modelled response is shown by the dotted line in figure 2(a). However, the sample fabrication process did not produce such a perfect surface; in reality some surface roughness is inevitable, in this case of the order of 5 μm. The solid line shows the predicted resonant frequency with the addition of a 5 μm surface roughness (h) on the teeth. This rough surface model clearly provides a far better fit to the data. The minimal change in resonant frequency from that of the plane slit is remarkable considering that 70% of the metal has been removed from the slit walls. Figure 2(b), computed from the FEM code, shows that it is strong confinement of the resonant electric fields into the slit region directly bounded by the

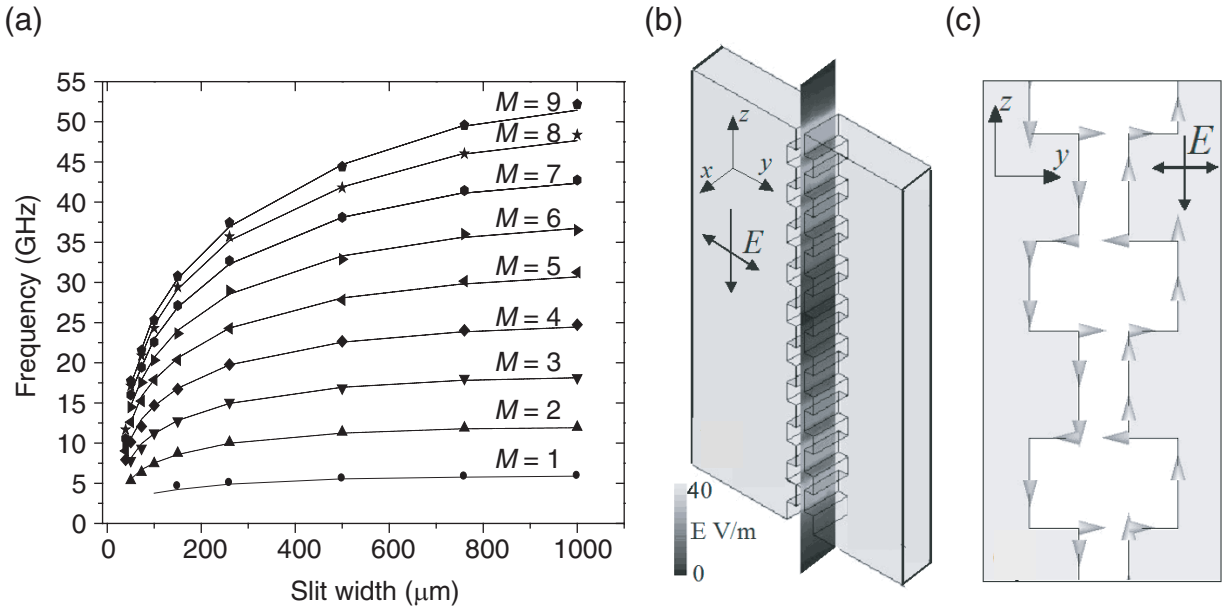

Figure 3. (a) Experimental data (shaped dots) showing resonant frequency for sample (b) as a function of slit width, over the range $0 < w_s < 1000\,\mu$m. Resonant modes $N = 1 - 9$ are shown where possible. FEM predictions are given by lines. (b) Computed electric field amplitudes for the $N = 1$ resonance with a slit width of 500 μm, within sample (b); shown in the x–z plane. Maximum field enhancement is about 40. (c) Instantaneous surface current, plotted in the y–z plane for same model sample (b).

teeth that gives this similarity in response. For the 8th order mode and a slot width of 73 μm an electric field enhancement of 20 times that of the field injected into the model is shown inside the slit.

Rotating the cuts so that they are parallel to the long axis of the slit produces a very different resonant frequency response to that shown in figure 2(a). Figure 3(a) shows the resonant frequencies of sample (b) as a function of slit width, over the range $50 < w_s < 1000\,\mu$m. The experimental data are shown as various shaped dots, depending on mode number, and the FEM modelled data as the various patterned lines. The resonant modes $1 < N < 9$ are shown over the range $0 < f < 55$ GHz. In stark contrast to figure 2, the resonant frequency of each mode is shown to be highly dependent on slit width, reducing in frequency, with decreasing slit width, until the lowest modes drop below the frequency range of the experimental apparatus (4.6 GHz). The $N = 9$ mode frequency is shown to reduce from 52.2 to 17.7 GHz as the slit width is reduced from 1000 to 50 μm. A resonant frequency of ~68 GHz is expected for a single slit in a perfect metal. Therefore, the cuts appear to make the slit respond as though it was filled with a meta-material with an enhanced refractive index. Furthermore, given that only the sample with the cuts made parallel to the long axis demonstrates this reduction in resonant frequency, the meta-material must be considered anisotropic; any enhancement of the refractive index occurs when waves propagate in a direction perpendicular to the cuts. This behaviour is explained by considering the field profiles at resonance.

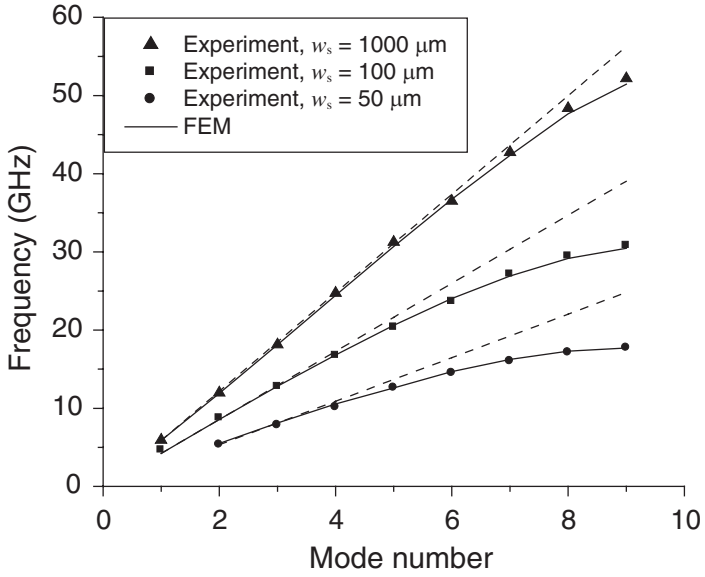

Figure 4. Resonant frequency as a function of resonant mode order for sample (b) with slit widths of 1000, 100 and 50 μm. Modes $N = 1 - 9$ are shown over frequency range $0 < f < 30$ GHz. Experimental data are shown as dots, the finite element model is represented by the solid lines and the dashed lines are the extrapolated gradient of the lower order modes.

Figures 3(b) and (c) show the computed resonant field amplitudes for sample (b). The electric field amplitude of the $N = 1$ mode, plotted along a short length of slit on the x–z plane, shown in figure 3(b), is superficially identical to that of the $N = 1$ mode in a slit in uncut metal plate. The electric field amplitude shows maxima at the open ends of the slit with some finer field structure due to the presence of the teeth and cuts. An enhancement of ~40 inside the slit is shown over that of the injected field. To distinguish between the resonant responses of the slit in uncut metal and sample (b), we must consider the surface current on the surface of the metal within sample (b). Figure 3(c) shows the instantaneous surface current at a phase of 0° in the y–z plane. While the net direction of current flow on each plate is as that expected for a simple slit, the modulation of the slit walls caused by the cuts creates inductive current loops, in the y–z plane, which would not otherwise exist. Given that the resonant frequency of a circuit composed of capacitors and inductors is given by $\omega = 1/\sqrt{LC}$, where L and C are representative of the inductive and capacitive elements respectively, it might be expected that the introduction of an inductance to an otherwise capacitive slit would cause the resonant frequency to reduce. Furthermore, reducing slit width, which increases the capacitance, would also increase the interaction of the partial current loops on opposing plates, increasing the inductance, and hence reducing the resonant frequency yet further. This is clearly shown in figure 3(a), the resonant frequency approaching zero as the slit width is reduced. It is apparent also from the fact that with the microwave electric field in the same direction in sample (a), which has only marginally altered resonant frequencies, that it is the direction of the magnetic field that is causing the change in apparent refractive index.

Figure 4 shows the frequency, for sample (b), of each resonant mode as a function of mode number. Experimental data (dots) are plotted for $1 < N < 9$ over the frequency range,

$0 < f < 30$ GHz for slit widths, $w_s = 50$, 150 and 1000 μm. The FEM modelled data are shown as the solid lines. It is clear that the lower order modes are separated equally in frequency, giving a linear response as predicted by Fabry–Perot theory. A linear fit to the lower order mode data yields a line whose gradient is in terms of GHz per mode number (dashed lines). From equation (1) this would be expected to be 7.5 GHz for a slit of depth of 20.01 mm filled with air. From this it is possible to calculate the effective refractive index of the interior of the slit and, given that $n = \sqrt{\varepsilon\mu}$ (ε being the relative permittivity and μ the relative permeability), the relative effective permeability may also be calculated, assuming that the effective relative permittivity is 1. The gradients of the linear fits indicate internal refractive indices of 1.2 ($\mu = 1.5$) for the 1000 μm slit width, 1.8 ($\mu = 3.3$) for the 150 μm slit width and 3.01 ($\mu = 9.1$) for the 50 μm slit width at low order mode numbers. However, as the mode number approaches $N = 10$, the separation of each of the modes decreases, for a given slit width, making the response flatten off. Hence, as the mode number increases the effective refractive indices also appear to increase; the group velocity of the photons within the slit at $N = 9$ is further reduced from that at mode $N = 1$. At $N = 9$, the refractive indices appear to be 1.3 ($\mu = 1.7$) for the 1000 μm slit width, 2.2 ($\mu = 4.8$) for the 150 μm slit width and 3.8 ($\mu = 14.4$) for the 50 μm slit width, a marked increase over that of the low order modes. The phase velocity of the photons within the cavity at the $N = 9$ mode are similarly reduced to $\sim 1/10$ of a slit in metal with no cuts. There is no $N = 10$ resonant mode observed; at this mode number the periodicity of the resonant fields within the slit becomes commensurate with the periodicity of the cuts, resulting in a resonance within the cuts themselves. This last resonant mode within the slit is the standing wave state at the bottom of a stop band which extends up in frequency to above the experimental frequency range (75 GHz).

As a further check on this effective increased index experiments were undertaken with both samples for changing angle of incidence. The resonant frequency of an unfilled, infinitely long single slit in metal will vary as $f_{FP}/\cos\theta$, where f_{FP} is a normal incidence Fabry–Perot resonant frequency and $\cos\theta$ is the angle of incidence [13]. This rise in frequency is due to the need to conserve photon momentum along the slit. It is to be expected that an anisotropic material within the slit will give a different response with increase of angle of incidence, one that is dependent on the orientation of the enhanced refractive index axis.

Figure 5 shows the angle dependent transmission of the sample with the cuts aligned perpendicular to the long axis of the slit (figure 1(a)). The data is shown over the frequency range $50 < f < 75$ GHz, angle range $\pm 80^\circ$ and a slit width of 500 μm. Recall that at normal incidence the sample transmits at the same resonant frequencies as an unfilled slit, figure 2(a). Here it is clear that the resonant frequency of each mode shown does not rise as $1/\cos\theta$ as expected for a simple slit. In fact, by considering the slit to be filled with a material which has an enhanced refractive index along its length, the resonant frequency can be simply shown to change as

$$f_0^2 = cN^2/2d/[1 - (\sin^2\theta/n_x^2)] \tag{2}$$

where n_x is the refractive index along the slit. Clearly as n_x increases, the resonant frequency of a mode decreases for any given angle of incidence. The rate of increase in resonant frequency as a function of angle, shown in figure 5, translates into a refractive index of 2.9 ± 0.1 ($\mu_x = 8.7 \pm 0.2$) along the long axis of the slit.

Similarly, figure 6 shows the transmission of the sample shown in figure 1(b), over the frequency range $5 < f < 9$ GHz, angle range of $\pm 70^\circ$ and a slit width of 250 μm. As the cuts

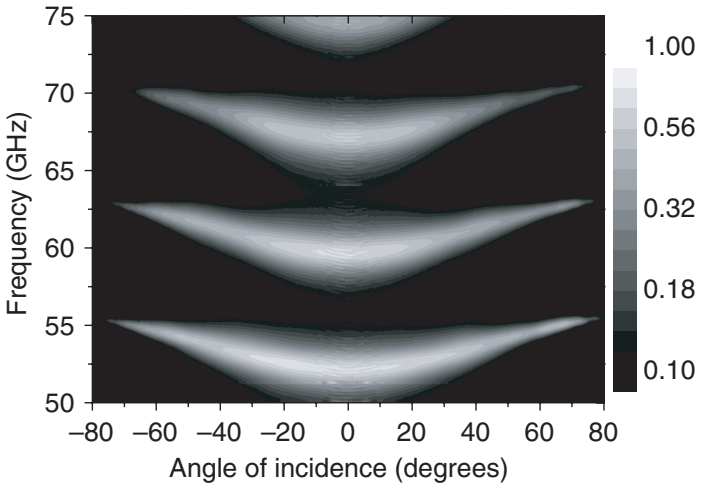

Figure 5. Experimental data showing resonant frequency as a function of angle for sample (a). Data are shown over frequency range $50 < f < 75\,\text{GHz}$ and angle range $-80^\circ < \theta < 80^\circ$. Slit dimensions: depth, $t = 20.01\,\text{mm}$, width, $w_s = 500\,\mu\text{m}$. Transmission intensity is shown on a logarithmic scale.

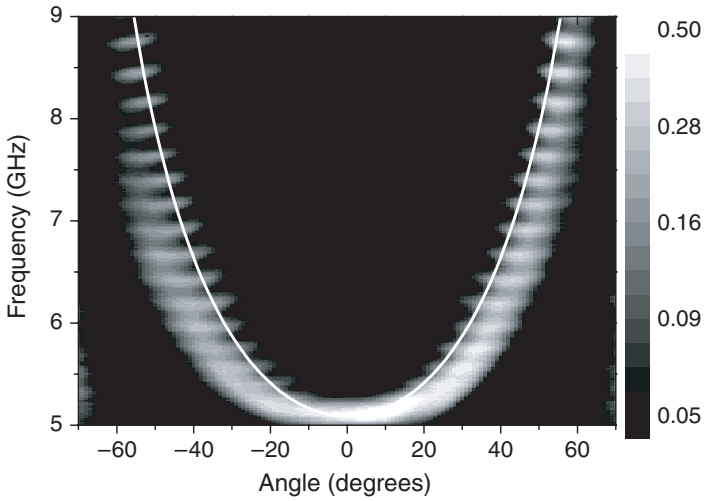

Figure 6. Experimental data showing the change in resonant frequency of the $N = 1$ mode as a function of angle for sample (b). Data are shown over frequency range $5 < f < 9\,\text{GHz}$ and angle range $-70^\circ < \theta < 70^\circ$. Slit width $= 250\,\mu\text{m}$. Prediction of equation (3) is shown as the white line with $\mu_z \approx 2.1$. Transmission intensity is shown on a logarithmic scale.

in this sample are parallel to the long axis of the slit, the refractive index associated with this direction is now expected to be $n_x = 1$. This is shown to be true as the frequency of the resonant mode rises as the white line, the form of which is given by

$$f_\theta = \left(\frac{cN}{2d}\right)\frac{1}{n_z}\frac{1}{\cos\theta}, \tag{3}$$

for a slit filled with a material with an enhanced refractive index along the short axis of the slit only (n_z). The mode shown is the fundamental resonance at 5.05 GHz. Given that this mode would be expected to be at 7.3 GHz, for a slit of width 250 μm, a refractive index of $\sim$1.45 ($\mu_z = 2.1$) is used to fit the simple function to the data. Overall, it can be seen that the trend of the main band is the same as for a slit in an uncut metal plate, demonstrating that the refractive index (and permeability) along the length of the slit is unity. (The slight deviation from the predicted trend at low angles of incidence is probably due to the inexact analogy of the cuts as an anisotropic medium.) This result verifies that the refractive index of a slit in which cuts are made into the metal will show an enhanced effective refractive index inside the slit in a direction perpendicular to the cuts. The banding of the mode is reminiscent of the sub-bands shown within finite length slits [13]. These would appear to arise from an interaction of the resonant modes with the periodicity of the teeth.

In summary, normal incidence resonant transmission of microwaves through a modulated single subwavelength slit in a metal plate has been recorded. It has been shown that subwavelength cuts made perpendicular to the long axis of the slit do not significantly change the resonant frequency of the slit from that of the uncut metal plate, despite the removal of 70% of the metal from the slit walls. In contrast, a slit with cuts made parallel to the long axis of the slit is shown to transmit microwaves at frequencies much reduced from that of the single slit in a metal plate. The creation of current loops around the cuts adds an inductive character to the structure, which might otherwise be considered largely capacitive. This results in a reduction of resonant frequency which is found to be proportional to the slit width. By measuring the frequency separation of the modes it is possible to determine the effective refractive index for each slit width. Refractive indices as high as 3.8 were recorded, equating to an effective relative permeability of 14.4. Further evidence of the anisotropy of the internal structure of the slit is presented as angle dependent data. Both samples are shown to display enhanced refractive index for propagation along a direction perpendicular to the cuts whilst for propagation in the orthogonal direction the index remains at unity.

Acknowledgments

We thank Mr P Cann for his assistance in the construction of the samples and both the Engineering and Physical Sciences Research Council (EPSRC) and the QinetiQ Fellow's Stipend Fund for their financial support.

References

[1] Porto J A, García-Vidal F J and Pendry J B 1999 *Phys. Rev. Lett.* **83** 2845
[2] Astilean S, Lalanne Ph and Palamaru M 2000 *Opt. Commun.* **175** 265
[3] Collin S, Pardo F, Teissier R and Pelouard J-L 2002 *J. Opt. A: Pure Appl. Opt.* **4** 154
[4] Went H E, Hibbins A P, Sambles J R, Lawrence C R and Crick A P 2000 *Appl. Phys. Lett.* **77** 2789
[5] Hibbins A P, Sambles J R, Lawrence C R and Robinson D M 2001 *Appl. Phys. Lett.* **79** 2844
[6] Takakura Y 2001 *Phys. Rev. Lett.* **86** 5601
[7] Yang F and Sambles J R 2002 *Phys. Rev. Lett.* **89** 063901

[8] Suckling J R, Sambles J R, Hibbins A P, Lockyear M J, Preist T W and Lawrence C R 2004 *Phys. Rev. Lett.* **92** 147401
[9] Bravo-Abad J, Martin-Moreno L and Garcia-Vidal F J 2004 *Phys. Rev. E.* **69** 026601
[10] Lindberg J, Lindfors K, Setälä T, Kaivola M and Friberg A T 2004 *Opt. Express* **12** 623
[11] Yang F and Sambles J R 2002 *J. Phys. D: Appl. Phys.* **35** 3049
[12] HFSS, Ansoft Corporation, Pittsburg, PA, USA
[13] Suckling J R, Hibbins A P, Sambles J R and Lawrence C R 2005 *New J. Phys* **7** 250